Energy Proceedings
Vol 52, 2025
ISSN 2004-2965

Analyzing the Optimal Voltage Range for Detecting Internal Short Circuits in Lithium-Ion Batteries#

ChiJyun Ko[1*], KuoChing Chen [2]

1 Institute of Applied Mechanics, National Taiwan University, 1, Sec. 4, Roosevelt Rd., Taipei 10617, Taiwan

2 Institute of Applied Mechanics, National Taiwan University, 1, Sec. 4, Roosevelt Rd., Taipei 10617, Taiwan
(Corresponding Author: d10543004@ntu.edu.tw)

ABSTRACT

Internal short circuit (ISC) is considered one of the main causes of battery failure, making early detection of ISC crucial for battery safety. The charging voltage curve contains abundant information about the battery state, reflecting various conditions, and is easily obtainable during the charging process. Therefore, it serves as an excellent signal for ISC detection. This research employs parallel resistor methods to simulate different leakage current scenarios and analyzes the impact of various charging voltage ranges on ISC. It identifies the optimal voltage range for detecting leakage current as 3.6 V to 3.7 V and determines that the resistance value capable of detecting the slightest ISC is 700 ohms. Furthermore, this method has been successfully applied in various environmental temperatures and series-connected battery packs, demonstrating its versatility across different scenarios.

Keywords: Lithium-ion battery, Internal short circuit, Partial charging, Constant current

1. INTRODUCTION

Lithium-ion batteries have been widely used in electric vehicles and energy storage systems. In recent years, ensuring the safety of batteries during operation has become an important research topic [1–3]. Among them, internal short circuit (ISC) is considered one of the main causes of battery failure. If an ISC occurs in the battery, it will not only cause a loss of capacity but also generate a large amount of heat, possibly leading to thermal runaway. Therefore, early detection of ISCs is crucial to prevent more serious dangers. This research explores how to detect early ISCs in batteries effectively.

In previous research on early ISC diagnosis methods, ISC detection can be categorized into two categories based on the battery's state, as shown in Table 1. The first category involves detection during the battery's charging and discharging process [4–10]. In this analysis, if the charging and discharging process involves dynamic current scenarios, detection is often conducted through equivalent circuit models (ECM) and filters. For example, Lai et al. [7] used an Extended Kalman Filter (EKF) to estimate the battery's state of charge (SOC) under dynamic current discharge conditions and further analyzed the battery's ISC level through the SOC differences between different batteries. On the other hand, if the charging and discharging process involves constant current scenarios, the dQ/dV curve can be used for analysis. For instance, Qiao et al. [5] quantified ISC by the shift of peaks in the incremental capacity (IC) curve.

Table 1 Methods for detecting ISC

	Ref.	Battery state	Feature	Maximum ISC_R (Ω)
	[4]	CC charge	IC curve	100
	[5]	CC charge	IC curve	1,000
	[6]	CC charge	Charge curve	1,000
1. Charging/ discharging process	[7]	Dynamic current	SOC variation	100
	[8]	Dynamic current	Discharge curve	100
	[9]	Dynamic current	Voltage curve	300
	[10]	Dynamic current	Discharge curve	1,000
	[11]	Relaxation state	Relaxation voltage	3,000
2. Resting process	[12]	Relaxation state	EIS	40
	[13]	Relaxation state	EIS	200

This is a paper for the 16th International Conference on Applied Energy (ICAE2024), Sep. 1-5, 2024, Niigata, Japan.

Detecting ISC during the battery's operation process can provide real-time reflection of the battery state, allowing for the early detection of potential problems, and ensuring battery safety.

The second category involves ISC detection during the battery's resting process [11–13]. This method can be divided into directly using relaxation voltage signals for detection. For example, Qiao et al. [11] measured relaxation voltage data at different time points and input it into a machine learning model to predict the battery's ISC level. Another approach is to apply external disturbances and measure the changes in electrochemical impedance spectroscopy (EIS) for ISC analysis. For example, Cui et al. [13] used low-frequency EIS signals as inputs to a machine learning model to analyze the battery's ISC. This approach often requires long-term data or additional EIS signals for analysis, making it more suitable for the classification and safety evaluation of retired batteries. For batteries in operation, these signals are difficult to obtain during the charging and discharging process.

In Table 1, we further summarize the ISC detection level of different signals (the larger the 〖ISC〗_R, the milder the corresponding ISC level). We can also observe that methods using voltage for detection can detect more minor leakage currents. Therefore, using voltage curves for internal short circuit analysis not only eliminates the need for additional operations on the battery but is also easier to implement in practical applications and can detect more minor leakage currents. In this research, we also select voltage information for internal short circuit analysis.

Given the advantages of voltage data, this research aims to utilize voltage curves from the charging phase for ISC analysis. The main contributions of this study can be summarized as follows:

1. ISC detection can be achieved using partial constant current charging data.

2. Analyzing the optimal voltage range for internal short circuit detection.

3. The analysis is feasible across different environmental temperatures and applicable within series-connected battery packs.

The remaining sections of the paper are organized as follows. Section 2 introduces the methodology for simulating experiments with varying degrees of ISC and analyzing voltage curves. Section 3 presents the results under different experimental conditions, such as environmental temperature and battery pack configurations. Finally, Section 4 provides the conclusions drawn from the results.

2. METHODOLOGY

2.1 Experimental

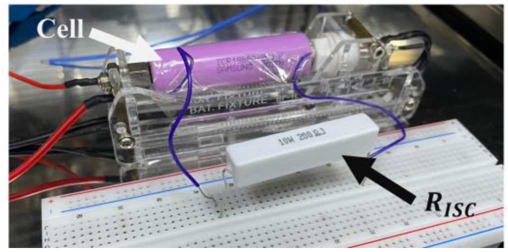

Fig. 1 Photo of ISC cell experiment

Due to the numerous possibilities of actual ISC occurrences, and the potential danger if a battery experiences an internal short circuit, conducting experiments may pose risks. In other words, simulating real ISCs presents significant challenges and potential hazards in experimental setups. Therefore, in recent years, to simulate the phenomenon of ISC, the common practice has been to parallel the battery with an external resistor. This approach is adopted due to the resemblance of electrical characteristics exhibited by external short circuits to early ISC within the battery. Our focus is on monitoring the variations in these electrical characteristics. The advantage of this method is that it eliminates the need for invasive experiments on the battery and allows for quantification of the severity of ISC through parallel resistor values. This research also adopts this method for simulating internal short circuits, as shown in Fig. 1.

In this research, we utilize battery data generated from commercially available 18,650-type NMC batteries with a nominal capacity of 2.6 Ah (Samsung ICR 18650-26J). The experiments use a charge/discharge cycling system (Bio-Logic BCS-815). Fig. 2 illustrates the charging process of batteries in parallel with different resistances from SOC=0% to 4.2 V at a constant current of 0.2C. The resistance values use in our experiments are 50 Ω, 100 Ω, 300 Ω, 500 Ω, 700 Ω, and the reference for the normal battery (labeled as ISC_{Inf} in the figure). It can be observed from the graph that as the parallel resistance decreases, the time taken to charge to 4.2V increases. This is attributed to smaller resistance values resulting in larger leakage currents in the battery, leading to varying degrees of charge loss and hence differences in charging time.

2.2 ISC diagnostic method

In Fig. 2, we observe differences in the charging curves corresponding to different degrees of ISC, and it

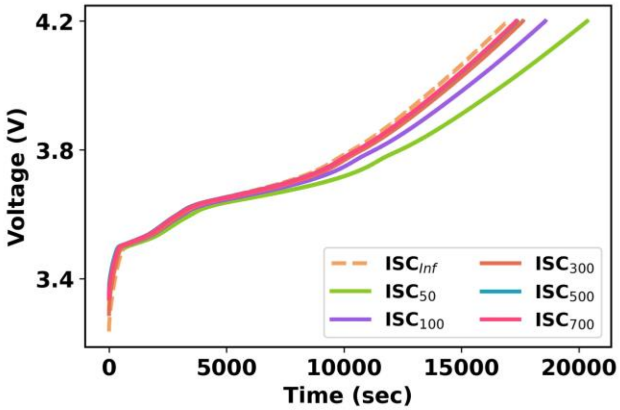

Fig. 2 CC charging voltage curves with different ISC resistances

is evident that not every voltage interval exhibits good discriminative ability. Therefore, to further analyze the optimal voltage range for detecting internal short circuits, we utilize the approach illustrated in Fig. 3.

In Fig. 3(a), the current curves for normal battery charging, charging with ISC, and leakage current during charging are displayed. From Fig. 3(b), it can be observed that although the charging curves start charging at the same time, the two curves reach V_n at different time points, denoted a $t_{n_k}^N$ and $t_{n_k}^I$, respectively. Additionally, the time taken for the voltage to rise to V_{n+dV} also differs between the two curves ($t_{n_{k+dV}}^N$, $t_{n_{k+dV}}^I$). Thus, it is evident from this figure that under the same charging voltage interval, normal batteries and those with ISC exhibit different charging times. We use the time difference recorded in different voltage intervals as an indicator for detecting internal short circuits.

The calculation method employed as follows:

$$T_{dif_{n_k}} = t_{n_{k+dV}} - t_{n_k}$$

Where t_{n_k} represents the time at which charging reaches V_k and $t_{n_{k+dV}}$ represents the time at which charging reaches V_{k+dV}.

In Fig. 3(c), we need to record the initial voltage value (V_{1_k}) and its corresponding times, $t_{1_k}^N$ and $t_{1_k}^I$. When the voltage rises to $V_{1_{k+dV}}$, the corresponding times are $t_{1_{k+dV}}^N$ and $t_{1_{k+dV}}^I$, and $t_{1_{k+dV}} - t_{1_k}$ represents $T_{dif_{1_k}}^N$

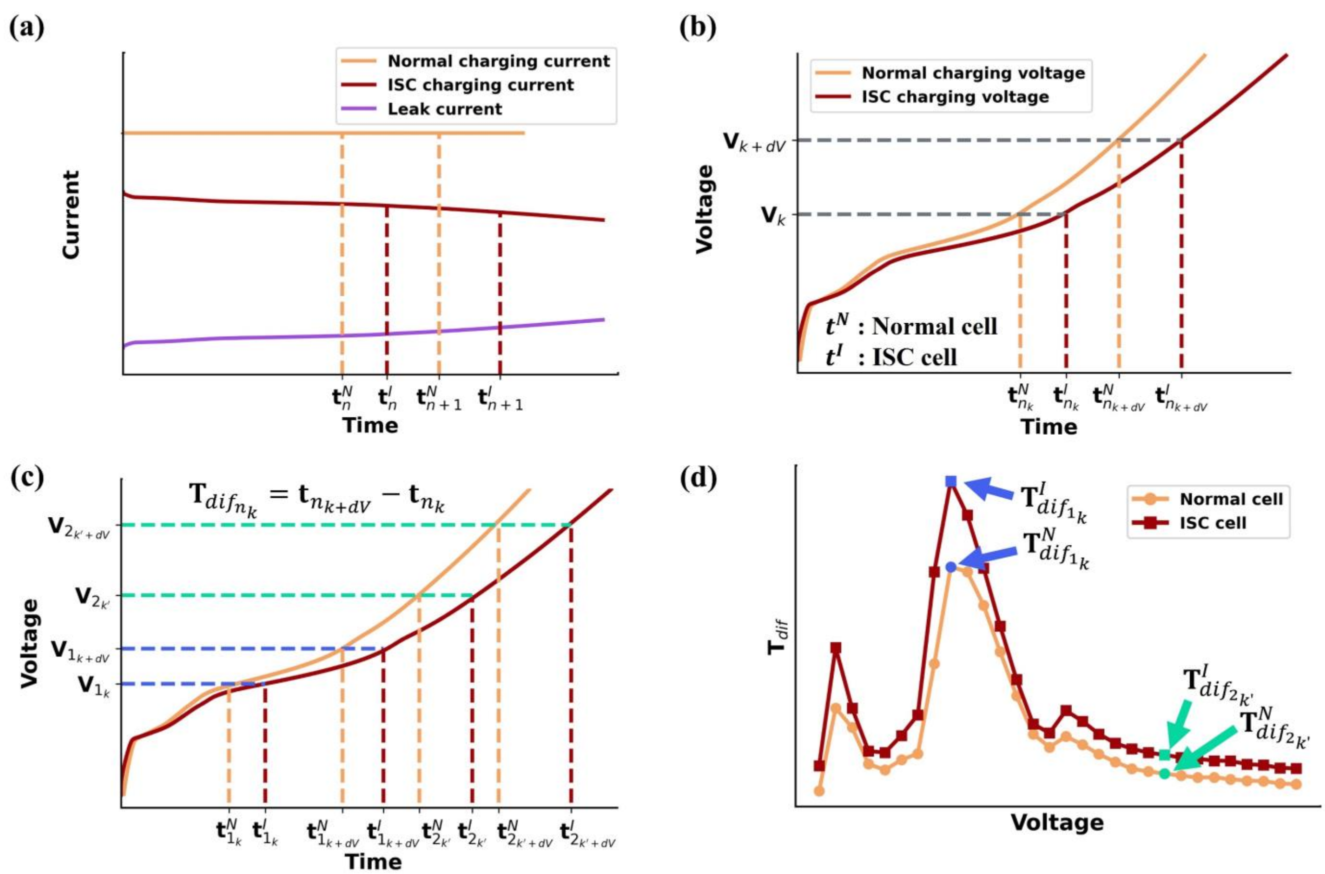

Fig. 3 Schematic of the proposed method for diagnosis ISC. (a) Analysis of charging current and leakage current. (b) CC charging voltage curves. (c) Differences in charging curves between normal battery and ISC battery. (d) The T_{dif} in various voltage ranges.

and $T^{I}_{dif_{1_k}}$. By analyzing the $T^{N}_{dif_{1_k}}$, $T^{I}_{dif_{1_k}}$ obtained during the same voltage rise segment, we can distinguish whether the battery exhibits a leakage current phenomenon.

In Fig. 3(d), $V_{k+dV} - V_k$ is set to the same difference value for all cases. The horizontal axis represents different V_k values during the charging stage, and the vertical axis represents $T_{dif_{n_k}}$ in different voltage intervals. From the graph, even with the same voltage difference, $T_{dif_{1_k}}$ can better identify whether the battery has an ISC phenomenon compared to $T_{dif_{2_k}}$ in different charging voltage ranges. Therefore, we further analyze the resolution in different charging voltage intervals to identify the optimal voltage range for recognizing internal short circuits in batteries.

3. RESULTS

3.1 Analysis of different voltage ranges

In Fig. 4(a), the values of T_{dif} across different voltage ranges are shown, where the voltage difference between V_k and V_{k+dV} is 0.01 V. It can be observed from the figure that around the voltage of approximately 3.65 V, T_{dif} exhibits significant differences under various parallel resistance conditions. However, in other voltage ranges, although the values of T_{dif} vary to different extents with ISC, they exhibit a trend of proximity. In Fig.4(b), we further analyze the differences in T_{dif} across different voltage ranges using the following equation:

$$P_{ISC^{I}_{n_k}} = \frac{T^{I}_{dif_{n_k}} - T^{N}_{dif_{n_k}}}{T^{N}_{dif_{n_k}}} \times 100\%$$

Where n represents different voltage ranges, $T^{I}_{dif_{n_k}}$ represents the T_{dif} of ISC batteries with different levels of ISC in different voltage ranges, and $T^{N}_{dif_{n_k}}$ represents the T_{dif} of a normal battery in different voltage ranges. Through this equation, we can obtain the proportion of the difference in T_{dif} between the ISC battery and the normal battery across different voltage ranges, thereby quantifying which voltage range shows the most significant difference. In Fig. 4(b), it can be

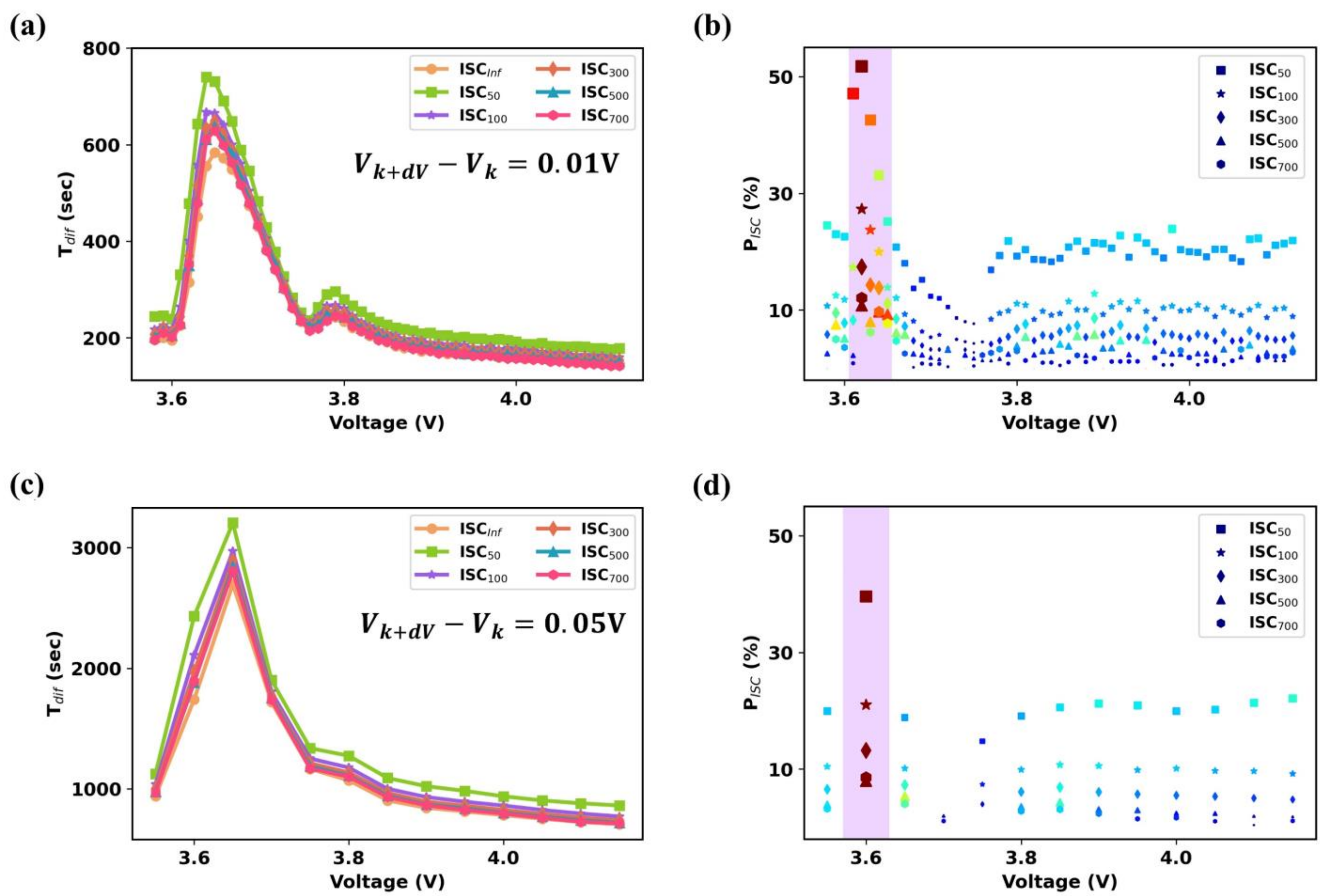

Fig. 4 (a) The T_{dif} for different voltage intervals with dv of 0.01. (b) The P_{ISC} results for dv of 0.01. (c) The T_{dif} for different voltage intervals with dv of 0.05. (d) The P_{ISC} results for dv of 0.05.

observed that when V_k is 3.62 V, there is a larger difference proportion compared to the normal battery. This indicates that in this voltage range, it is easier to identify whether the battery has generated a leakage current.

In Fig. 4(c), we adjust the voltage difference $V_{k+dV} - V_k$ to 0.05 V. It can be observed from the figure that even with this adjustment, the trend of T_{dif} remains very similar to that in Fig. 4(a), with a noticeable difference around the 3.65 V range. Using the above equation for further analysis, Fig. 4(d) also shows a significant percentage difference between ISC batteries and normal batteries in the 3.6 V range. Therefore, even when different voltage differences are used for analysis, similar trends are observed. From the above results, it can be concluded that T_{dif} varies across different voltage ranges, and there is a more significant difference when the battery is charged between 3.6 V and 3.7 V. Therefore, using data from this voltage range can more effectively detect ISC in batteries.

3.2 Different charging condition

In Fig. 4, we identify the optimal voltage range for detecting leakage current to be between 3.6 V and 3.7 V. To validate the applicability of this method, we apply it under different conditions in this section, including (i) various ambient temperatures and (ii) identification within a series-connected battery pack.

3.2.1 Various ambient temperatures

First, under different ambient temperatures, we conduct experiments with the battery in a 10°C incubator. Fig. 5(a) shows the voltage curve obtained using 0.2C CC charging. Fig. 5(b) shows T_{dif} across different voltage ranges. From the figure, we can see results similar to those at room temperature, with noticeable differences in the charging curves for different levels of ISC around 3.67 V. This indicates that the method is effective under varying ambient temperatures.

3.2.2 Series-connected battery pack

Next, we conduct experiments with two batteries connected in series. As shown in Fig. 5(c), one battery is

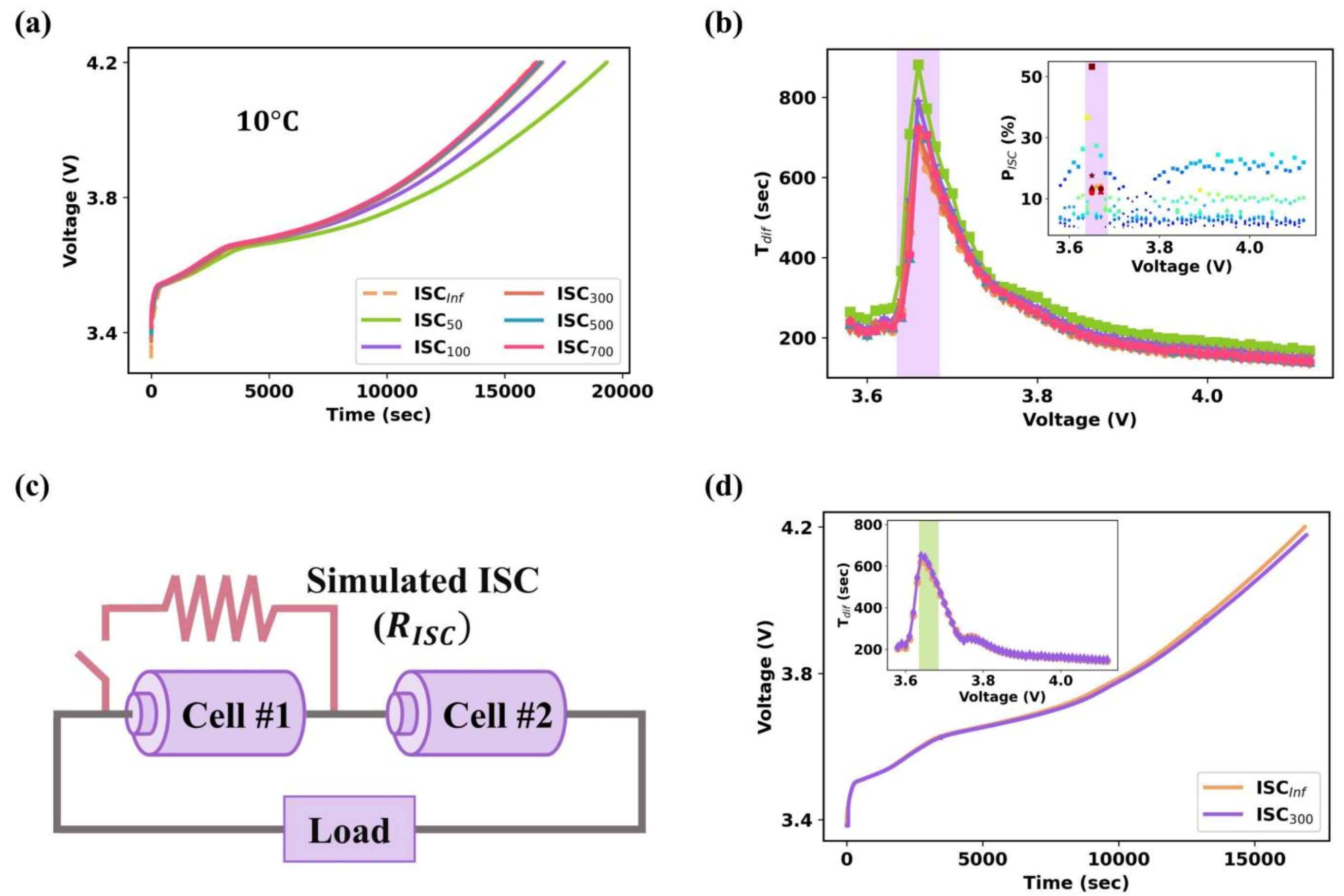

Fig. 5 (a) CC charging curves at an ambient temperature of 10°C. (b) The T_{dif} results at an ambient temperature of 10°C. (c) Schematic of series-connected battery pack. (d) CC charging curves and T_{dif} results in series-connected batteries.

connected with a parallel resistor to simulate ISC, while the other battery is a normal battery. Fig. 5(d) shows the differences in the charging curves during a single charging process. It can be observed that the voltage rise trend of the ISC_{300} battery is slower than that of the normal battery. The top left corner of Figure 5(d) also exhibits significant differences at 3.65 V. From these results, we can conclude that as long as the voltage of individual cells can be measured, this method can also be applied to series-connected batteries for analysis.

4. CONCLUSIONS

Since the charging voltage curve can reflect the leakage current phenomenon of a battery, this research detects ISC in batteries by analyzing the characteristics of the charging curve. The features of this method are as follows: (i) It requires only partial charging curve data to detect ISC. (ii) It identifies the optimal charging range for ISC detection and can detect the most minor ISC condition with a parallel resistor of 700 ohms. (iii) This method can be applied to different ambient temperatures and series-connected battery packs, enhancing its practical applicability. In future research, we will extend this method to analyze batteries with varying health conditions, different charging currents, and different parallel resistor values, aiming to further expand its application scope.

ACKNOWLEDGEMENT

This work was supported by the National Science and Technology Council R.O.C. under Grant NSTC 112–2221–E–002–253–MY3

REFERENCE

[1] Lai X, Jin C, Yi W, Han X, Feng X, Zheng Y, Ouyang M. Mechanism, modeling, detection, and prevention of the internal short circuit in lithium-ion batteries: Recent advances and perspectives. Energy Stor Mater 2021;35:470–499.

[2] Song Y, Park S, Kim S W. Model-free quantitative diagnosis of internal short circuit for lithium-ion battery packs under diverse operating conditions. Applied Energy 2023;352:121931.

[3] Zhang W, Ouyang N, Yin X, Li X, Wu W, Huang L. Data-driven early warning strategy for thermal runaway propagation in Lithium-ion battery modules with variable state of charge. Appl Energy 2022;323:119614.

[4] Sun J, Chen S, Xing S, Guo Y, Wang S, Wang R, Wu Y, Wu X. A battery internal short circuit fault diagnosis method based on incremental capacity curves. J Power Sources 2024;602:234381.

[5] Qiao D, Wang X, Lai X, Zheng Y, Wei X, Dai H. Online quantitative diagnosis of internal short circuit for lithium-ion batteries using incremental capacity method. Energy 2022;243:123082.

[6] Fan W, Qiao D, Lai X, Zheng Y, Wei X, Dai H. A novel method of quantitative internal short circuit diagnosis based on charging electric quantity in fixed voltage window. J Energy Storage 2023;70;108096.

[7] Lai X, Yi W, Kong X, Han X, Zhou L, Sun T, Zheng Y. Online detection of early stage internal short circuits in series-connected lithium-ion battery packs based on state-of-charge correlation. J Energy Storage 2020;30;101514.

[8] Ma R, Deng Y, Wang X. Simplified electrochemical model assisted detection of the early-stage internal short circuit through battery aging. J Energy Storage 2023;66: 107478.

[9] Zhu G, Sun T, Xu Y, Zheng Y, Zhou L. Identification of internal short-circuit faults in lithium-ion batteries based on a multi-machine learning fusion. Batteries 2023;9(3);154.

[10] Qiao D, Wei X, Jiang B, Fan W, Gong H, Lai X, Zhrng Y, Dai H. Data-Driven Fault Diagnosis of Internal Short Circuit for Series-Connected Battery Packs Using Partial Voltage Curves. IEEE Trans Industr Inform 2024;20(4):6751–6761.

[11] Qiao D, Wei X, Jiang B, Fan W, Lai X, Zheng Y, Dai H. Quantitative Diagnosis of Internal Short Circuit for Lithium-Ion Batteries Using Relaxation Voltage. IEEE Trans Ind Electron 2024; 1–10.

[12] Ma R, He J, Deng Y. Investigation and comparison of the electrochemical impedance spectroscopy and internal resistance indicators for early-stage internal short circuit detection through battery aging. J Energy Storage 2022;54:105346.

[13] Cui B, Wang H, Li R, Xiang L, Du J, Zhao H, Li S, Zhao X, Yin G, Cheng X, Ma Y, Huo H, Zuo P, Du C. Internal short circuit early detection of lithium-ion batteries from impedance spectroscopy using deep learning. J Power Sources 2023;563:232824.